Bioactive Constituents, Metabolites, and Functions

Extracellular Glutamate-Induced mTORC1 Activation via the IR/IRS/PI3K/ Akt Pathway Enhances the Expansion of Porcine Intestinal Stem Cells

Min Zhu, Ying-chao Qin, Chun-qi Gao, Hui-chao Yan, Xiang-guang Li, and Xiu-qi Wang

Just Accepted

Glu induced mTORC1 activation in the intestinal epithelium. Glu activates mTORC1 through the IR/IRS/PI3K/Akt signaling pathway and promotes intestinal stem cell expansion. The expression of EAAT3, T1R1/T1R3, mGluR2/3, GATOR2, GATOR1, RagA, and v-ATPase did not change after extracellular Glu stimulation.

Title: Extracellular Glutamate-Induced mTORC1 Activation via the IR/IRS/PI3K/Akt Pathway Enhances the Expansion of Porcine Intestinal Stem Cells

Min Zhu,[†] Ying-chao Qin,[†] Chun-qi Gao,[†] Hui-chao Yan,[†] Xiang-guang Li,*,[‡] and Xiu-qi Wang,*,[†]

† College of Animal Science, South China Agricultural University/Guangdong Provincial Key Laboratory of Animal Nutrition Control/National Engineering Research Center for Breeding Swine Industry, Guangzhou 510642, China

‡ Department of Pharmaceutical Engineering, School of Biomedical and Pharmaceutical Sciences, Guangdong University of Technology, Guangzhou 510006, China

* Correspondence author: Xiang-guang Li, email: xgli@gdut.edu.cn;

Xiu-qi Wang, email: xqwang@scau.edu.cn.

ABSTRACT

Glutamate (Glu) is a critical nutritional regulator of intestinal epithelial homeostasis. In addition, intestinal stem cells (ISCs) at crypt bases are known to play important roles in maintaining the renewal and homeostasis of the intestinal epithelium, and the aspects of communication between Glu and ISCs are still unknown. Here, we identify Glu and mammalian target of rapamycin complex 1 (mTORC1) as essential regulators of ISC expansion. The results showed that extracellular Glu promoted ISC expansion, indicated by increased intestinal organoid forming efficiency and budding efficiency as well as cell proliferation marker Ki67 immunofluorescence and differentiation marker Keratin 20 (KRT20) expression. Moreover, the insulin receptor (IR) mediating phosphorylation of the insulin receptor substrate (IRS) and downstream signaling phosphoinositide 3-kinase (PI3K)/protein kinase B (Akt) pathway was involved in this response in ISCs. As expected, Glu-induced mTORC1 signaling activation was observed in the intestinal porcine enterocyte cell line (IPEC-J2), and Glu activated the PI3K/Akt/mTORC1 pathway. Accordingly, PI3K inhibition partially suppressed Glu-induced mTORC1 activation. In addition, Glu increased the phosphorylation levels of IR and IRS, and inhibiting IR downregulated the IRS/PI3K/Akt pathway. Collectively, our findings first indicate that extracellular Glu activates mTORC1 via the IR/IRS/PI3K/Akt pathway and stimulates ISC expansion, providing a new perspective for regulating the growth and health of the intestinal epithelium.

KEYWORDS: mTORC1, IR/IRS/PI3K/Akt, glutamate, intestinal stem cells, organoid

INTRODUCTION

Glutamate (Glu) is one of the most abundant amino acids in dietary proteins (approximately 15-45%)[1] and is notably the main contributor to intestinal energy consumption, which involves protein synthesis and oxidative energy supply.[2] Furthermore, as a functional amino acid, Glu extensively participates in intraluminal nutrient metabolic regulation[3] and plays crucial roles in intestinal epithelial proliferation,[4-5] intestinal integrity,[6] animal growth performance,[7] intestinal development and whole-body homeostasis in mammals.[8-9] Therefore, Glu nutrition is garnering increasing attention.[10]

Intestinal stem cells (ISCs), located at the base of the crypt, are responsible for intestinal epithelial self-renewal and intestinal epithelial homeostasis throughout an organisms lifespan.[11] The signaling pathways involved in the regulation of ISC activity include Wnt, bone morphogenetic protein (BMP), Notch, mammalian target of rapamycin complex 1 (mTORC1) and epidermal growth factor (EGF),[12-14] and a specific microenvironment (stem cell niche) is required for ISCs to maintain their stemness and function properly.[11] Therefore, culturing ISCs *in vitro* is challenging. ISCs generated from crypts developed into organoids *in vitro* by simulating the niche of ISCs *in vivo*.[15] The *ex vivo* organoid models in humans and mice have been well established and widely used in fundamental research.[16-17] Furthermore, porcine intestinal organoid cultivation has also been reported recently in our laboratory, and the culture system is different from those of mice and humans.[18] However, the nutritional manipulation of porcine ISC expansion *in vitro* has yet to be illuminated. Moreover, little is known about Glu nutrition and ISCs and the underlying mechanism.

48   In early research, mTORC1 has been demonstrated to regulate cell growth and

49   metabolism in response to changes in amino acid levels. Of course, mTORC1 is also

50   associated with growth factors, energy and other nutrients.[19] Furthermore, previous

51   studies have suggested that the pathway upstream of mTORC1 is complex.[20] Growth

52   factors, such as insulin and insulin-like growth factor (IGF), initiate downstream

53   signaling through the phosphorylation of insulin receptor substrate (IRS) to activate

54   the phosphatidylinositol 3-kinase (PI3K)/protein kinase B (Akt)/tuberous sclerosis

55   complex (TSC) pathway and induce mTORC1 activation.[21]

56   However, recent studies have suggested that amino acids, particularly arginine and

57   leucine, sense intracellular signals and transmit these signals to mTORC1 through

58   specific receptors in the cytoplasm or lysosomal membranes in HEK293T cells.[22-25]

59   Interestingly, different amino acids have distinct sensors,[22, 24] and mTORC1 is

60   activated in different manners in the presence of the same amino acid.[23-24] Moreover,

61   GAP activity toward Rags 2/1 (GATOR2/1) and RagA GTPase is required for

62   arginine- and leucine-induced mTORC1 activation.[22, 24] Therefore, the mechanism of

63   Glu sensing in intestinal epithelial cells and the mechanism by which communication

64   with mTORC1 governs stem cell activity has provoked our attention.

65   In our previous studies, Glu deficiency and inhibition of its major transporter

66   (excitatory amino acid transporter 3 (EAAT3)) were shown to markedly suppress

67   mTORC1 activity.[4-5] Here, we show that porcine intestinal organoids, grown from the

68   expansion of intestinal crypts, are a suitable *ex vivo* model to study intestinal cell

69   physiology and function. In this study, we determined the effect of Glu on ISC

70   expansion and mTORC1 activation and further investigated the underlying

71   mechanism of Glu signaling cascades in porcine intestinal organoids and IPEC-J2

72   cells. We demonstrated that Glu activated mTORC1 signaling via the

73   IR/IRS/PI3K/Akt signaling pathway. In addition, Glu promoted ISC expansion,

74   providing new insights into the Glu nutritional regulation of intestinal growth and

75   health.

MATERIALS AND METHODS

Porcine crypt isolation and culture

Porcine intestinal crypts were isolated and cultured as described previously.[18] Briefly, the jejuna of 7-day-old piglets (*Landrace × Yorkshire*) was opened longitudinally, washed with ice-cold Dulbecco's phosphate-buffered saline (DPBS) and cut into 3-5 mm pieces; the segment was almost immediately soaked in 30 mM ethylenediaminetetraacetic acid disodium salt (EDTA, Sigma-Aldrich, St. Louis, MO, USA) in an ice bath for 30 min. Then, the supernatant was discarded, and fresh DPBS was added; the solution was changed every 5 min until high-purity crypts were acquired.

Collected crypts were embedded in Matrigel (BD Biosciences, San Jose, CA，USA), seeded in a 48-well plate (Corning, Corning, NY, USA) and incubated at 37℃ for 20 min. Then, complete culture medium was added, which included nearly 90% WRN (Wnt3a, noggin, and R-spondin 1) conditioned medium, 10% fetal bovine serum (FBS), 100 U/mL penicillin-100 μg/mL streptomycin, 1× N2 supplement (Invitrogen, Carlsbad, CA, USA), 1 mM N-acetylcysteine (Sigma-Aldrich), 10 mM nicotinamide (Sigma-Aldrich), 50 ng/mL recombinant murine EGF (PeproTech, Rocky Hill, NJ, USA), 10 μM Y27632 (Stemgent, Cambridge, MA, USA), 1× B27 supplement (Invitrogen), 0.5 μM LY2157299 (Selleck, Houston, TX, USA), 10 μM SB202190 (Sigma-Aldrich), and 10 μM CHIR99021 (Stemgent). The crypts were cultured to obtain organoids. The organoid forming efficiency was the ratio of the organoid number to the number of crypts seeded, and the organoid budding efficiency was a ratio of the budding organoid number to the total organoid number.

All animal procedures were performed in accordance with the Guidelines for the Care and Use of Laboratory Animals of South China Agricultural University (Guangzhou,

101 China), and experiments were approved by the Animal Ethics Committee of South

102 China Agricultural University.

Automated capillary Western blotting (WES)

104 WES, a new automatic protein expression quantitative analysis system for ultramicro

105 samples, was introduced to detect the expression of proteins in intestinal organoids.

106 All operations were performed strictly according to the user guide. In brief, after

107 lysing the organoids in RIPA lysis buffer, the protein lysates were diluted, mixed with

108 5× fluorescence masters and a biotinylated ladder, boiled for 5 min, and stored on ice.

109 The lysates and other reagents were dispensed onto the assay plate. The plate was

110 loaded into the instrument, and the WES assay protocol was configured to run

111 automatically. The data were analyzed by Compass software 3.1 (Protein Simple, San

112 Jose, CA, USA). The results were confirmed by 3 independent experiments with 3

113 samples per group.

Cells and cell culture

115 IPEC-J2 cells, an intestinal porcine enterocyte cell line, were derived from the jejuna

116 of newborn piglets and cultured in high-glucose Dulbecco's Modified Eagle's

117 Medium (DMEM, Thermo Fisher Scientific, 12800-017, Waltham, MA, USA)

118 supplemented with 10% FBS, Gibco, 10099-141, Waltham, MA, USA) and 1%

119 penicillin/streptomycin (Gibco, 10378016). Cultures were maintained in a humidified

120 incubator at 37°C in 5% CO_2. The medium was replaced every other day. All

121 experiments were performed on cells at passages 8-12.

Cell treatment

123 At the beginning of the treatment, IPEC-J2 cells were cultured in DMEM without

124 FBS for 15 h and then in an amino acid-starved Hank's balanced salt solution (HBSS,

125 Gibco, 24020117) and vitamin mixture (Sigma-Aldrich, St. Louis, MO, USA) for 4 h.

126 IPEC-J2 cells were incubated with 5 mM glutamate (Sigma-Aldrich) for different

127 amounts of time (0, 10, 20, 30, 60, and 120 min) to establish the optimal treatment

128 time. Next, the cells were divided into the control, Glu treatment, inhibitor treatment,

129 and Glu + inhibitor treatment groups. The PI3K inhibitors wortmannin and LY294002

130 (Selleck Chemicals, Houston, TX, USA) or the IR inhibitors GSK1838705A and

131 linsitinib (Selleck Chemicals) were used in this study. All experiments were repeated

132 three times.

133 **Western blotting**

134 IPEC-J2 cells were collected for Western blotting analysis as previously described.[26]

135 Briefly, proteins were isolated from the cells, separated by 10% sodium dodecyl

136 sulfate-polyacrylamide gel electrophoresis (SDS-PAGE) and transferred onto

137 polyvinylidene difluoride (PVDF) membranes (Millipore, Burlington, MA, USA).

138 After blocking with 5% skim milk for 1 h, the membranes were incubated with

139 primary antibodies (1:1000 dilution) overnight at 4°C and then with secondary

140 antibodies (1:5000 dilution) for 2 h. The proteins were visualized using a Beyo ECL

141 Plus chemiluminescence detection kit (Beyotime Institute of Biotechnology,

142 Shanghai, China) on a FluorChem M imaging system (Protein Simple, San Jose, CA,

143 USA). ImageJ software (version 1.8.0 112, National Institute of Health, Bethesda,

144 MD, USA) was used to analyze the band densities, and the results were confirmed by

145 3 independent experiments with 3 samples per group.

146 The following antibodies were used in this study: anti-mTOR (#2972),

147 anti-phospho-mTOR (Ser2448, #5536), anti-S6K1 (#9202), anti-phospho-S6K1

148 (Thr389, #9205), anti-S6 (#2708), anti-phospho-S6 (Ser235/236, #9234), anti-TSC2

149 (#4308), anti-Akt (#9272), anti-phospho-Akt (Thr308, #13038), anti-PI3K (#4257),

150 anti-phospho-PI3K (Tyr458, #4228), anti-IRS-1 (#3407), anti-phospho-IRS-1

151 (Ser636, #2388), Mios (#13557), NPRL2 (#37344), and RagA (#4357) from Cell

152 Signaling Technology (Beverly, MA, USA); p-IR (Tyr1150/1151, sc-81500) and IR

153 (sc-57342) from Santa Cruz Biotechnology; ATP6V1B2 (ab-73404) from Abcam;

154 and anti-β-actin (AP0060), anti-rabbit IgG (BS13278) and anti-goat IgG (BS30503)

155 antibodies from Bioworld Technology (Louis Park, MN, USA).

156 **Real-time PCR**

157 The cells were collected for real-time PCR as previously described.[27] mRNA

158 abundance (n = 6) was determined by real-time PCR using a Stratagene Mx3005P

159 qPCR system (Agilent Technologies, Santa Clara, CA, USA) and SYBR Green

160 Real-Time PCR Master Mix (Toyobo, Osaka Prefecture, Japan). The specific primer

161 pairs used are detailed in Table S1. Melting curve analysis was conducted to confirm

162 the specificity of each product, and product sizes were verified using ethidium

163 bromide-stained 1.5% agarose gels in Tris acetate-EDTA buffer. Quantitative data

164 were obtained using the $2^{-\Delta\Delta Ct}$ method. The experiments were performed in triplicate.

165 **Immunofluorescence confocal microscopy**

166 Organoids and cells were seeded in 48-well culture plates (Corning, #3599, New

167 York, NY, USA) and treated as previously described.[27] Then, the organoids and cells

168 were fixed with 4% paraformaldehyde for 30 min, permeabilized with 0.3% Triton

169 X-100 for 15 min and blocked in a protein solution (Dako, Santa Clara, CA, USA) for

170 20 min. The primary antibodies (1:200 dilution) listed above were incubated with the

171 organoids and cells overnight at 4℃. Cy3-conjugated secondary antibody (1:500

172 dilution in antibody diluent; Jackson, Jackson, USA) staining was performed at room

173 temperature for 2 h. Nuclei were stained with 4'6-diamidino-2-phenylindole (DAPI,

174 1:1000 dilution in PBS; Sigma-Aldrich) for 10 min at room temperature. Fluorescence

175 signals were observed with a Nikon A1R HD25 confocal microscope (NIS-Elements,

176 Nikon, Melville, NY, USA). Three independent experiments were performed.

177 **Statistical analysis**

178 Data are presented as the mean ± SEM. The data were analyzed using SPSS software

179 version 20.0 (SPSS Inc., Chicago, IL, USA). Variance analysis was performed with

180 Student's t-test or one-way analysis of variance followed by a least significant

181 difference test. Differences between groups were considered statistically significant at

182 $P < 0.05$.

183   **RESULTS**

184   **Glu promotes the *ex vivo* expansion of porcine intestinal stem cells**

185   To determine the effects of Glu on porcine ISC expansion, the porcine intestinal

186   organoid culture medium was supplemented with 2 or 5 mM Glu. The organoid

187   forming efficiency and budding efficiency were determined on days 4 and 6,

188   respectively. As shown in Figure 1A, crypts were viable and developed into intestinal

189   organoids with typical crypt-villus structures; moreover, the 5 mM Glu group showed

190   a better growth pattern than the other groups. The supplementation of either 2 mM or

191   5 mM Glu increased ($P<0.05$) the intestinal organoid forming efficiencies and

192   budding efficiencies compared with those in the control group (Figure 1B, 1C). In

193   addition, the organoid budding efficiency of the 5 mM Glu group was greater

194   ($P<0.05$) than that of the 2 mM Glu group (Figure 1C). Therefore, 5 mM Glu was

195   chosen in the following experiments. Furthermore, the 5 mM Glu group exhibited

196   enhanced ISC activity compared with that in the control group as determined by cell

197   proliferation marker Ki67 staining (Figure 1D) and assessment of the differentiation

198   marker Keratin 20 (KRT20) (Figure 1E, 1F). Taken together, these results indicated

199   that Glu is an essential nutrient that enhances the *ex vivo* expansion of porcine ISCs.

200   **Glu activates mTORC1 and IR/IRS/PI3K/Akt signaling in porcine organoids**

201   To investigate the possible involvement of the mTORC1 and IR/IRS/PI3K/Akt

202   signaling pathways in the ISC expansion response to Glu, organoids from the control

203   and 5 mM Glu groups were harvested at day 6, and the levels of proteins related to

204   these signaling pathways were determined by WES. The results in Figure 2 show that

205   the protein levels of p-mTOR (Ser2448) and its downstream and upstream proteins

206   p-S6K1 (Thr389), p-S6 (Ser235/236), p-IR (Tyr1150/1151), p-IRS (Ser636), p-PI3K

207   (Tyr458) and p-Akt (Thr308) were significantly increased ($P<0.05$) in the 5 mM Glu

208   organoids, whereas the TSC2 level was obviously decreased ($P<0.05$). Furthermore,

209   the organoids were subjected to immunofluorescence staining with p-mTOR

210   (Ser2448), p-S6K1 (Thr389), p-S6 (Ser235/236), p-PI3K (Tyr458), p-Akt (Thr308)

211   and TSC2 antibodies. The expression patterns of these proteins between groups were

212   consistent with the WES results. These data suggest that the mTORC1 and

213   IR/IRS/PI3K/Akt signaling pathways are involved in the ISC expansion response to

214   Glu. To further elucidate the underlying mechanisms, we adopted IPEC-J2 for the

215   following experiments.

216   **Glu activates the mTORC1 pathway**

217   To explore the mTORC1 pathway response to the Glu treatment time, IPEC-J2 cells

218   were treated with 5 mM Glu for different amounts of time (0, 10, 20, 30, 60, and 120

219   min). The cells were then collected for protein extraction and determination of the

220   levels of key proteins in the mTORC1 pathway. Compared with those in the control

221   group, the protein levels of p-mTOR (Ser2448), p-S6K1 (Thr389) and p-S6

222   (Ser235/236) peaked at 60 min after Glu treatment (Figure 3B, 3C, $P<0.05$).

223   Collectively, Glu activated the mTORC1 signaling pathway. Therefore, IPEC-J2 cells

224   were treated with 5 mM Glu for 60 min in the following experiments.

225   **Glu activates the PI3K/Akt pathway**

226   To illustrate the intensive mechanism by which mTORC1 senses Glu, the levels of

227   protein upstream of mTORC1, including p-PI3K (Tyr458), PI3K, p-Akt (Thr308),

228   Akt, and TSC2, were analyzed. The p-PI3K (Tyr458) and p-Akt (Thr308) levels

229   (Figure 4A, 4B) were significantly increased, and the TSC2 level (Figure 4A, 4B) was

230   significantly decreased ($P<0.05$). In addition, the cell immunofluorescence staining

231   results (Figure 4C-4H) of p-PI3K (Tyr458), p-Akt (Thr308), TSC2, p-mTOR

232   (Ser2448), p-S6K1 (Thr389) and p-S6 (Ser235/236) were in agreement with those of

233 the Western blotting assay, indicating that PI3K/Akt/TSC2 signaling was associated

234 with the Glu-induced activation of mTORC1.

Glu-induced mTORC1 activation is reduced by the PI3K inhibitor

236 To confirm that Glu activates mTORC1 through the PI3K/Akt signaling pathway,

237 IPEC-J2 cells were serum- and amino acid-starved and then divided into control, Glu

238 treatment, wortmannin treatment, wortmannin + Glu treatment, LY294002 treatment,

239 and LY294002 + Glu treatment groups. Western blotting (Figure 4A, 4B) and

240 immunofluorescence staining (Figure 4C-4H) showed that the p-PI3K (Tyr458),

241 p-Akt (Thr308), p-mTOR (Ser2448), p-S6K1 (Thr389), and p-S6 (Ser235/236) levels

242 were decreased in the wortmannin + Glu and LY294002 + Glu groups compared with

243 those in the Glu group, and the TSC2 expression level was accordingly increased

244 ($P<0.05$). Furthermore, a greater inhibitory effect was observed upon treatment with

245 50 μM LY294002 compared to that achieved with 500 nM wortmannin under Glu

246 treatment conditions ($P<0.05$). However, the PI3K inhibitor (wortmannin and

247 LY294002) + Glu group still activated the PI3K/Akt/mTORC1 pathway compared

248 with that observed in the inhibitor (wortmannin and LY294002) group ($P<0.05$). In

249 summary, these results suggested that PI3K inhibition partially reduced the levels of

250 Glu-induced mTORC1 activation.

Glu induces mTORC1 activation through the IR/IRS pathway

252 The PI3K/Akt pathway was shown to function upstream of mTORC1 signaling in

253 Glu-induced mTORC1 activation, and we wanted to further clarify whether IR/IRS

254 signaling is involved in this process. First, we evaluated the phosphorylation of IR

255 and IRS. As shown in Figure 6A-B, Glu significantly increased the p-IR

256 (Tyr1150/1151) and p-IRS (Ser636) expression levels ($P<0.05$). We next used two

257 different IR inhibitors, GSK1838705A and linsitinib, to analyze the phosphorylation

258   of IR, IRS, PI3K, and Akt. p-IR (Tyr1150/1151), p-IRS (Ser636), p-PI3K (Tyr458),

259   and p-Akt (Thr308) (Figure 6C, 6D) were significantly decreased in the

260   GSK1838705A + Glu and linsitinib + Glu groups compared with those in the Glu

261   group ($P<0.05$), indicating that GSK1838705A and linsitinib decreased Glu-induced

262   IR/IRS/PI3K/Akt signaling activation. Additionally, the Glu group also activated

263   IR/IRS/PI3K/Akt signaling compared with that observed in the inhibitor

264   (GSK1838705A and linsitinib) alone group ($P<0.05$).

265   **A Glu transporter, Glu receptors and GATOR2/GATOR1/Rag GTPase signaling**

266   **are not linked to Glu-induced mTORC1 activation**

267   To determine whether a Glu transporter and receptors are involved in Glu-induced

268   mTORC1 activation, we determined the mRNA abundance of the Glu transporter

269   EAAT3, and taste receptor type 1-member (T1R) 1/3 (T1R1/3) and metabotropic

270   glutamate receptor 2/3 (mGluR2/3), possible Glu-sensing receptors, were also

271   observed. However, the mRNA abundances of those genes did not change (Figure

272   7A). GAP activity toward Rags 2/1 (GATOR2/1) and RagA GTPase are required for

273   arginine- and leucine-induced mTORC1 activation. Therefore, we also determined the

274   levels of Mios (GATOR2), NPRL2 (GATOR1), RagA, and ATP6V1B2 (v-ATPase)

275   expression. Unexpectedly, the levels of these proteins also did not change (Figure 7B

276   and C).

DISCUSSION

ISCs are critical for maintaining intestinal epithelial homeostasis (a high-turnover tissue).[28-29] Moreover, multiple reports have also demonstrated crucial roles of Glu in intestinal epithelial homeostasis.[9-10] Organoids with organotypic properties provide an ideal platform for simulating the natural environment *in vivo*.[30] The current study used *ex vivo* porcine jejunal organoids to assess the role of Glu in the regulation of ISC activity, as Glu was previously shown to accelerate ISC division and promote gut growth via the mGluR in *Drosophila*, it also indicates that other regulatory pathways exsit.[8] We found that extracellular Glu also promoted porcine ISC expansion through IR. The insulin signaling pathway is indispensable for ISC proliferation,[31] and continuously activated IR accelerates ISC expansion, indicating that IR signaling can regulate ISC activity in agreement with metabolic adaptation to nutrition.[32] Increasing evidence suggests that IR activation is essential for feeding-induced ISC division and gut growth response.[33] Additionally, mTORC1 also mediates ISC function,[34] and as expected, our results further showed that Glu activated mTORC1 signaling in ISCs and stimulated the IR/IRS/PI3K/Akt pathway. There is evidence that the downstream mediators of insulin signaling include IRS, PI3Kinase, Akt, TSC2, and mTORC1.[35] Therefore, we used IPEC-J2 to confirm the relationship between the IR/IRS/PI3K/Akt pathway and mTORC1 signaling.

mTORC1 is a crucial regulator of many basic physiological metabolic processes, including anabolic and catabolic processes, and its dysregulation is involved in the progression of diseases.[20] mTORC1 is sensitive to changes in amino acid availability.[36] Unlike leucine and arginine, which have long been reported to be important for mTORC1 activation,[22, 24] the mechanisms of other amino acids in mTORC1 activation remain unknown. To investigate the conditions of Glu-induced

302 mTORC1 activation, we screened for the optimal treatment time using the intestinal

303 porcine enterocyte cell line IPEC-J2. In this study, we showed that Glu effectively

304 increased mTORC1 activity within 60 min, while both arginine and leucine activated

305 mTORC1 within only 10 min by amino acid restimulation.[22, 24] Additionally,

306 glutamine also activated mTORC1 within 60 min.[37] One possible explanation for the

307 discrepant results is that different amino acids affect mTORC1 activity to varying

308 degrees depending on different experimental conditions.

309 PI3K is an intracellular phosphatidylinositol kinase that can be activated by a series of

310 growth factors. Activated PI3K accelerates the phosphorylation of Akt, and PI3K/Akt

311 signaling pathways regulate mTORC1 signaling through the TSC complex, which is a

312 negative regulator.[38] Our results are consistent with this observation. The

313 phosphorylation of PI3K and Akt was upregulated sequentially, and the TSC2

314 complex was downregulated by Glu treatment. Furthermore, we showed that the

315 phosphorylation of PI3K, Akt, mTOR, S6K1, and S6 was reduced after treatment with

316 the PI3K inhibitors wortmannin and LY294002 under Glu supplementation. These

317 results further confirmed that Glu activates mTORC1 via the PI3K/Akt signaling

318 pathway.

319 Further studies were conducted to elucidate the elements upstream of PI3K. The

320 binding of a ligand to IR, a transmembrane heterotetrameric tyrosine kinase receptor,

321 facilitates the autophosphorylation of IR tyrosine residues. Activation of the receptor

322 leads to the recruitment of IRS-1, which activates the PI3K/Akt pathway.[39] The

323 phosphorylation of regulators upstream of PI3K, including IR and IRS, was also

324 markedly upregulated. Moreover, we used the specific IR inhibitors GSK1838705A

325 and linsitinib to confirm the results, and we showed that the inhibitors partially

326 eliminated the effect of Glu-induced IR/IRS/PI3K/Akt pathway activation. Therefore,

327 our study demonstrated that the IR/IRS/PI3K/Akt pathway is involved in mTORC1

328 activation after Glu stimulation. EAAT3 is considered the most important Glu

329 transporter in the intestine and promotes glutamate transport into cells.[5] In addition,

330 EAAT3 inhibition suppresses intestinal growth.[40] We hypothesized that EAAT3

331 might be a transceptor of glutamate to activate mTORC1, but EAAT3 expression was

332 not altered under Glu treatment in the current study. G protein-coupled receptors

333 (GPCRs) such as T1R 1/3 can act as amino acid sensors to transmit signals to

334 mTORC1.[41-42] We determined the levels of the GPCRs T1R 1/3 and mGluR 2/3,

335 which were not changed under Glu treatment.

336 The sensing of amino acids and then activation of mTORC1 are complicated.[43]

337 Cytoplasmic arginine, leucine and S-adenosylmethionine are sensed by CASTOR1,[22]

338 Sestrin2,[24, 44] and SAMTOR,[45] respectively; amino acid sensing signaling through the

339 GATOR2 and GATOR1 proteins is sequential,[46] and the signal converges to the Rag

340 GTPases. However, glutamine activates mTORC1 through Arf GTPase.[37] Member 9

341 of the solute carrier family 38 (SLC38A9) serves as a transceptor to sense lysosomal

342 arginine level changes, directly transmitting changes in the amino acid level to Rag

343 GTPases.[47] As mentioned earlier, amino acids in the cytoplasm can initiate mTORC1

344 activation by GATOR2/GATOR1 signaling. GATOR2 is the key hub of amino acid

345 sensing, where amino acid signals converge upstream of Rag GTPases to regulate

346 mTORC1 activity.[44] Unfortunately, our results showed that Glu did not change the

347 expression of Mios (a core component of GATOR2), NPRL2 (a core component of

348 GATOR1), or RagA. In addition, v-ATPase is an evolutionarily conserved proton

349 pump that senses amino acid levels,[48] and its expression is also invariable. Therefore,

350 the GATOR2/GATOR1/Rags pathway was not required for Glu-induced mTORC1

351   activation. In addition, we can conclude that other mechanisms of intracellular Glu

352   sensing and signal transmission exist.

353   In summary, our study elucidated the effects of Glu and nutrient-sensing signaling

354   pathways on ISCs and demonstrated that the IR/IRS/PI3K/Akt pathway is involved in

355   mTORC1 activation after Glu stimulation. Moreover, Glu was shown to further

356   promote ISC expansion (Figure 8). These findings are potentially applicable in the

357   study of intestinal development and health.

AUTHOR INFORMATION

Corresponding Authors

* E-mail for Xiang-guang Li: xgli@gdut.edu.cn;

* E-mail for Xiu-qi Wang: xqwang@scau.edu.cn; Tel/Fax: 86-20-38295462

ORCID

Xiang-guang Li: 0000-0002-1374-1444

Xiu-qi Wang: 0000-0003-2033-9485

Notes

The authors declare no conflict of interest.

Supporting Information Available: Supplemental table of primers used for quantitative real-time PCR

REFERENCE

(1) Alonso, S.; Yilmaz, O. H., Nutritional regulation of intestinal stem cells. *Annu Rev Nutr* **2018,** *38*, 273-301.

(2) Reeds, P. J.; Burrin, D. G.; Stoll, B.; Jahoor, F., Intestinal glutamate metabolism. *J Nutr* **2000,** *130* (4), 978s-982s.

(3) Brosnan, J. T.; Brosnan, M. E., Glutamate: a truly functional amino acid. *Amino Acids* **2013,** *45* (3), 413-8.

(4) Li, X. G.; Sui, W. G.; Gao, C. Q.; Yan, H. C.; Yin, Y. L.; Li, H. C.; Wang, X. Q., L-Glutamate deficiency can trigger proliferation inhibition via down regulation of the mTOR/S6K1 pathway in pig intestinal epithelial cells. *J Anim Sci* **2016,** *94* (4), 1541-1549.

(5) Ye, J. L.; Gao, C. Q.; Li, X. G.; Jin, C. L.; Wang, D.; Shu, G.; Wang, W. C.; Kong, X. F.; Yao, K.; Yan, H. C.; Wang, X. Q., EAAT3 promotes amino acid transport and proliferation of porcine intestinal epithelial cells. *Oncotarget* **2016,** *7* (25), 38681-38692.

(6) Jiao, N.; Wu, Z. L.; Ji, Y.; Wang, B.; Dai, Z. L.; Wu, G. Y., L-Glutamate enhances barrier and antioxidative functions in intestinal porcine epithelial cells. *J Nutr* **2015,** *145* (10), 2258-2264.

(7) Rezaei, R.; Knabe, D. A.; Tekwe, C. D.; Dahanayaka, S.; Ficken, M. D.; Fielder, S. E.; Eide, S. J.; Lovering, S. L.; Wu, G. Y., Dietary supplementation with monosodium glutamate is safe and improves growth performance in postweaning pigs. *Amino Acids* **2013,** *44* (3), 911-923.

(8) Deng, H. S.; Gerencser, A. A.; Jasper, H., Signal integration by Ca^{2+} regulates intestinal stem-cell activity. *Nature* **2015,** *528* (7581), 212.

(9) Hou, Y. Q.; Wu, G. Y., Nutritionally nonessential amino acids: a misnomer in nutritional sciences. *Adv Nutr* **2017,** *8* (1), 137-139.

(10) Hou, Y. Q.; Wu, G. Y., L-Glutamate nutrition and metabolism in swine. *Amino Acids* **2018,** *50* (11), 1497-1510.

(11) Barker, N., Adult intestinal stem cells: critical drivers of epithelial homeostasis and regeneration. *Nat Rev Mol Cell Biol* **2014,** *15* (1), 19-33.

(12) Sailaja, B. S.; He, X. C.; Li, L. H., The regulatory niche of intestinal stem cells. *J Physiol-London* **2016,** *594* (17), 4827-4836.

(13) Liang, S. J.; Li, X. G.;Wang, X. Q., Notch signaling in mammalian intestinal stem cells: maintaining homeostasis and determining cell fate. *Curr Stem Cell Res Ther* **2019,** DOI:10.2174/1574888X14666190429143734.

(14) Zhou, J. Y.; Huang, D. G.; Qin, Y. C.; Li, X. G.; Gao, C. Q.; Yan, H. C.; Wang, X. Q., mTORC1 signaling activation increases intestinal stem cell activity and promotes epithelial cell proliferation. *J Cell Physiol* **2019**. DOI: 10.1002/jcp.28542.

(15) Sato, T.; Vries, R. G.; Snippert, H. J.; van de Wetering, M.; Barker, N.; Stange, D. E.; van Es, J. H.; Abo, A.; Kujala, P.; Peters, P. J.; Clevers, H., Single Lgr5 stem cells build crypt-villus structures *in vitro* without a mesenchymal niche. *Nature* **2009,** *459* (7244), 262-U147.

(16) Wang, F. C.; Scoville, D.; He, X. C.; Mahe, M. M.; Box, A.; Perry, J. M.; Smith, N. R.; Lei, N. Y.; Davies, P. S.; Fuller, M. K.; Haug, J. S.; McClain, M.; Gracz, A. D.; Ding, S.; Stelzner, M.; Dunn, J. C. Y.; Magness, S. T.; Wong, M. H.; Martin, M. G.; Helmrath, M.; Li, L. H., Isolation and characterization of intestinal stem cells based on surface marker combinations and colony-formation assay. *Gastroenterology* **2013,** *145* (2), 383.

(17) Yin, X. L.; Farin, H. F.; van Es, J. H.; Clevers, H.; Langer, R.; Karp, J. M., Niche-independent high-purity cultures of Lgr5(+) intestinal stem cells and their progeny. *Nat Methods* **2014,** *11* (1), 106.

(18) Li, X. G.; Zhu, M.; Chen, M. X.; Fan, H. B.; Fu, H. L.; Zhou, J. Y.; Zhai, Z. Y.; Gao, C. Q.; Yan, H. C.; Wang, X. Q., Acute exposure to deoxynivalenol inhibits porcine enteroid activity via suppression of the Wnt/beta-catenin pathway. *Toxicol Lett* **2019,** *305*, 19-31.

(19) Gonzalez, A.; Hall, M. N., Nutrient sensing and TOR signaling in yeast and mammals. *Embo J* **2017,** *36* (4), 397-408.

(20) Saxton, R. A.; Sabatini, D. M., mTOR signaling in growth, metabolism, and disease. *Cell* **2017,** *169* (2), 362-362.

(21) Gross, S. M.; Rotwein, P., Mapping growth-factor-modulated Akt signaling dynamics. *J Cell Sci* **2016,** *129* (10), 2052-2063.

(22) Chantranupong, L.; Scaria, S. M.; Saxton, R. A.; Gygi, M. P.; Shen, K.; Wyant, G. A.; Wang, T.; Harper, J. W.; Gygi, S. P.; Sabatini, D. M., The CASTOR proteins are arginine sensors for the mTORC1 pathway. *Cell* **2016,** *165* (1), 153-164.

(23) Han, J. M.; Jeong, S. J.; Park, M. C.; Kim, G.; Kwon, N. H.; Kim, H. K.; Ha, S. H.; Ryu, S. H.; Kim, S., Leucyl-tRNA synthetase is an intracellular leucine sensor for the mTORC1-signaling pathway. *Cell* **2012,** *149* (2), 410-424.

(24) Wolfson, R. L.; Chantranupong, L.; Saxton, R. A.; Shen, K.; Scaria, S. M.; Cantor, J. R.; Sabatini, D. M., Metabolism sestrin2 is a leucine sensor for the mTORC1 pathway. *Science* **2016,** *351* (6268), 43-48.

(25) Wang, S. Y.; Tsun, Z. Y.; Wolfson, R. L.; Shen, K.; Wyant, G. A.; Plovanich, M. E.; Yuan, E. D.; Jones, T. D.; Chantranupong, L.; Comb, W.; Wang, T.; Bar-Peled, L.; Zoncu, R.; Straub, C.; Kim, C.; Park, J.; Sabatini, B. L.; Sabatini, D. M.,

Lysosomal amino acid transporter SLC38A9 signals arginine sufficiency to mTORC1. *Science* **2015,** *347* (6218), 188-194.

(26) Li, X. G.; Wang, Z.; Chen, R. Q.; Fu, H. L.; Gao, C. Q.; Yan, H. C.; Xing, G. X.; Wang, X. Q., Lgr5 and Bmi1 increase pig intestinal epithelial cell proliferation by stimulating Wnt/beta-catenin signaling. *Int J Mol Sci* **2018,** *19* (4), 1036.

(27) Fan, H. B.; Zhai, Z. Y.; Li, X. G.; Gao, C. Q.; Yan, H. C.; Chen, Z. S.; Wang, X. Q., CDX2 stimulates the proliferation of porcine intestinal epithelial cells by activating the mTORC1 and Wnt/-catenin signaling pathways. *Int J Mol Sci* **2017,** *18* (11), 2447.

(28) Andersson-Rolf, A.; Zilbauer, M.; Koo, B. K.; Clevers, H., Stem cells in repair of gastrointestinal epithelia. *Physiology* **2017,** *32* (4), 278-289.

(29) Zwick, R. K.; Ohlstein, B.; Klein, O. D., Intestinal renewal across the animal kingdom: comparing stem cell activity in mouse and *Drosophila*. *Am J Physiol-Gastr L* **2019,** *316* (3), G313-G322.

(30) Olayanju, A.; Jones, L.; Greco, K.; Goldring, C. E.; Ansari, T., Application of porcine gastrointestinal organoid units as a potential *in vitro* tool for drug discovery and development. *J Appl Toxicol* **2019,** *39* (1), 4-15.

(31) Biteau, B.; Hochmuth, C. E.; Jasper, H., Maintaining tissue homeostasis: dynamic control of somatic stem cell activity. *Cell Stem Cell* **2011,** *9* (5), 402-411.

(32) Karpac, J.; Younger, A.; Jasper, H., Dynamic coordination of innate immune signaling and insulin signaling regulates systemic responses to localized DNA damage. *Dev Cell* **2011,** *20* (6), 841-854.

(33) O'Brien, L. E.; Soliman, S. S.; Li, X. H.; Bilder, D., Altered modes of stem cell division drive adaptive intestinal growth. *Cell* **2011,** *147* (3), 603-614.

(34) Zhou, Y.; Rychahou, P.; Wang, Q.; Weiss, H. L.; Evers, B. M., TSC2/mTORC1 signaling controls paneth and goblet cell differentiation in the intestinal epithelium. *Cell Death Dis* **2015,** *6*, e1631.

(35) Boucher, J.; Kleinridders, A.; Kahn, C. R., Insulin receptor signaling in normal and insulin-resistant states. *Csh Perspect Biol* **2014,** *6* (1), a009191.

(36) Ham, D. J.; Lynch, G. S.; Koopman, R., Amino acid sensing and activation of mechanistic target of rapamycin complex 1: implications for skeletal muscle. *Curr Opin Clin Nutr* **2016,** *19* (1), 67-73.

(37) Jewell, J. L.; Kim, Y. C.; Russell, R. C.; Yu, F. X.; Park, H. W.; Plouffe, S. W.; Tagliabracci, V. S.; Guan, K. L., Differential regulation of mTORC1 by leucine and glutamine. *Science* **2015,** *347* (6218), 194-198.

(38) Kim, J.; Kim, E., Rag GTPase in amino acid signaling. *Amino Acids* **2016,** *48* (4), 915-928.

(39) Ward, C.; Lawrence, M.; Streltsov, V.; Garrett, T.; McKern, N.; Lou, M. Z.; Lovrecz, G.; Adams, T., Structural insights into ligand-induced activation of the insulin receptor. *Acta Physiol* **2008,** *192* (1), 3-9.

(40) Li, X. G.; Sui, W. G.; Yan, H. C.; Jiang, Q. Y.; Wang, X. Q., The *in ovo* administration of L-trans pyrrolidine-2,4-dicarboxylic acid regulates small intestinal growth in chicks. *Animal* **2014,** *8* (10), 1677-1683.

(41) Wauson, E. M.; Lorente-Rodriguez, A.; Cobb, M. H., Minireview: Nutrient sensing by G protein-coupled receptors. *Mol Endocrinol* **2013,** *27* (8), 1188-97.

(42) Zhou, Y.; Ren, J.; Song, T.; Peng, J.; Wei, H., Methionine regulates mTORC1 via the T1R1/T1R3-PLCbeta-Ca^{2+}-ERK1/2 signal transduction process in C2C12 Cells. *Int J Mol Sci* **2016,** *17* (10), 1684.

(43) Shimobayashi, M.; Hall, M. N., Multiple amino acid sensing inputs to mTORC1. *Cell Res* **2016,** *26* (1), 7-20.

(44) Chantranupong, L.; Wolfson, R. L.; Orozco, J. M.; Saxton, R. A.; Scaria, S. M.; Bar-Peled, L.; Spooner, E.; Isasa, M.; Gygi, S. P.; Sabatini, D. M., The sestrins interact with GATOR2 to negatively regulate the amino-acid-sensing pathway upstream of mTORC1. *Cell Rep* **2014,** *9* (1), 1-8.

(45) Gu, X.; Orozco, J. M.; Saxton, R. A.; Condon, K. J.; Liu, G. Y.; Krawczyk, P. A.; Scaria, S. M.; Harper, J. W.; Gygi, S. P.; Sabatini, D. M., SAMTOR is an S-adenosylmethionine sensor for the mTORC1 pathway. *Science* **2017,** *358* (6364), 813-818.

(46) Bar-Peled, L.; Chantranupong, L.; Cherniack, A. D.; Chen, W. W.; Ottina, K. A.; Grabiner, B. C.; Spear, E. D.; Carter, S. L.; Meyerson, M.; Sabatini, D. M., A tumor suppressor complex with GAP Activity for the Rag GTPases that signal amino acid sufficiency to mTORC1. *Science* **2013,** *340* (6136), 1100-1106.

(47) Shen, K.; Sabatini, D. M., Ragulator and SLC38A9 activate the Rag GTPases through noncanonical GEF mechanisms. *Proc Natl Acad Sci USA* **2018,** *115* (38), 9545-9550.

(48) Yang, H. R.; Gong, R.; Xu, Y. H., Control of cell growth: Rag GTPases in activation of TORC1. *Cell Mol Life Sci* **2013,** *70* (16), 2873-2885.
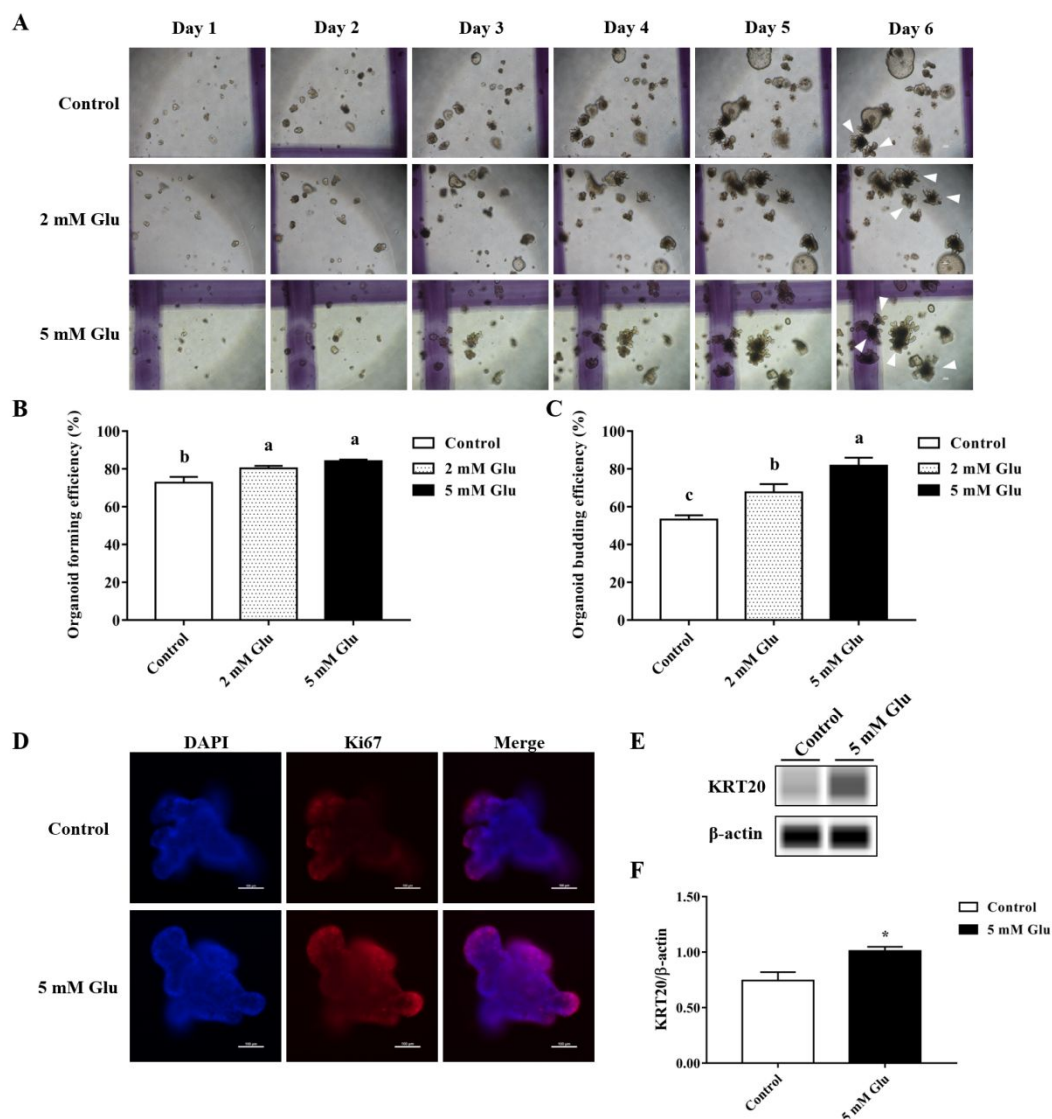
Figure 1. Glu was necessary for the expansion of intestinal stem cells *ex vivo*.

A-C. Glu stimulated organoid expansion. A. Organoid growth pattern, budding of organoids are indicated by white triangles. Scale bar: 100 μm. B. Forming efficiency of organoid. C. Budding efficiency of organoid. D. Representative immunofluorescence images of control or 5 mM Glu-treated organoids labeled with DAPI (blue) and a Ki67 antibody (red). Scale bar: 100 μm. E, F. The protein expression of KRT20 was analyzed in the intestinal organoid by WES. β-actin was used as a loading control. The results are representative of three independent

experiments and are reported as the mean ± SEM. * indicates $P<0.05$. In the bar charts, different superscript small letters indicate significant differences ($P < 0.05$), while the same letters represent no significant difference ($P > 0.05$).
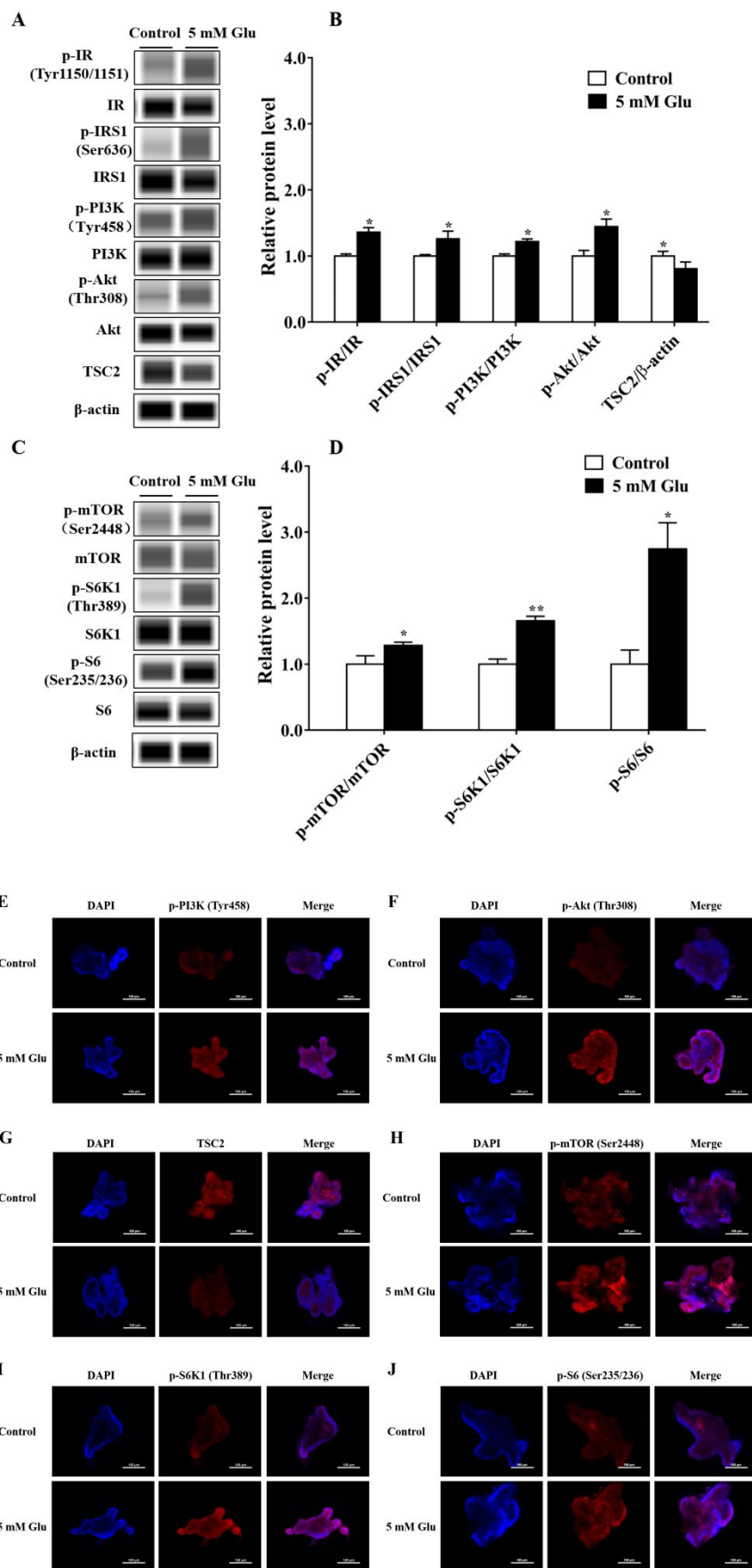
Figure 2. Glu activated mTORC1 and IR/IRS/PI3K/Akt signaling in intestinal stem cells. A-D. The protein expression of p-IR, IR, p-IRS1, IRS1, p-PI3K, PI3K, p-Akt, Akt, TSC2, p-mTOR, mTOR, p-S6K1, S6K1, p-S6, and S6 was analyzed in the intestinal organoid by WES. The results are representative of three independent experiments and are reported as the mean ± SEM. * indicates $P<0.05$, and ** indicates $P < 0.01$. E-J. Representative immunofluorescence images of control or 5 mM Glu-treated organoids labeled with DAPI (blue) and target protein antibodies (red). Scale bar: 100 μm.
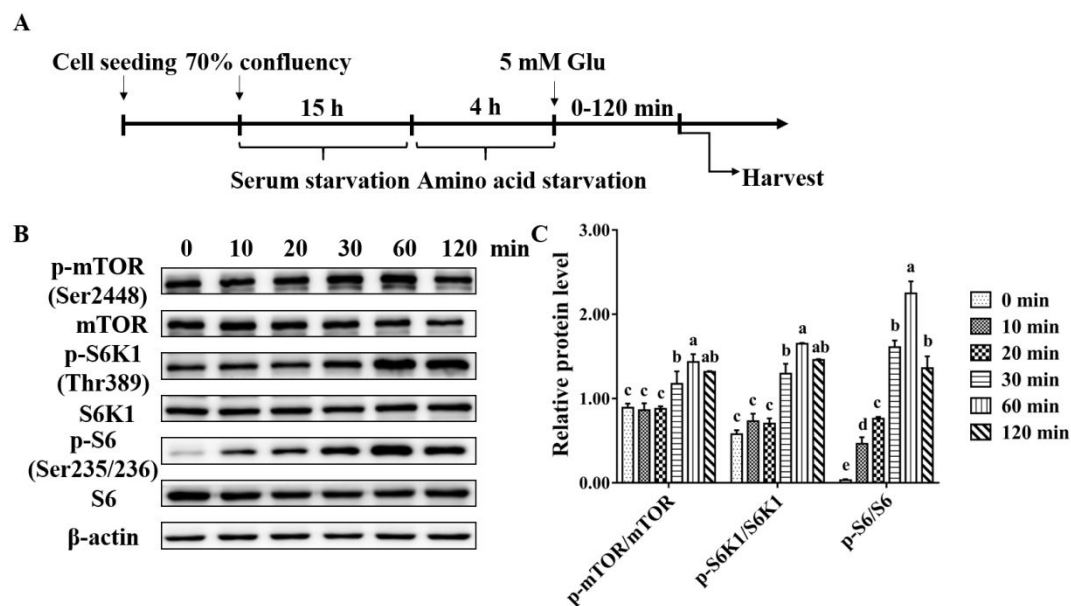
Figure 3. Glu induced mTORC1 activation. A. Experimental procedure. IPEC-J2 cells were serum-starved for 15 h, amino acid-starved for 4 h and then treated with 5 mM Glu for different amounts of time. B. The levels of p-mTOR, p-S6K1, and p-S6 were analyzed by Western blotting. C. Quantification was performed by measuring the intensity of each band by densitometry using ImageJ software. The results are representative of three independent experiments and are reported as the mean ± SEM. In the bar charts, different superscript small letters indicate significant differences ($P < 0.05$), while the same letters represent no significant difference ($P > 0.05$)
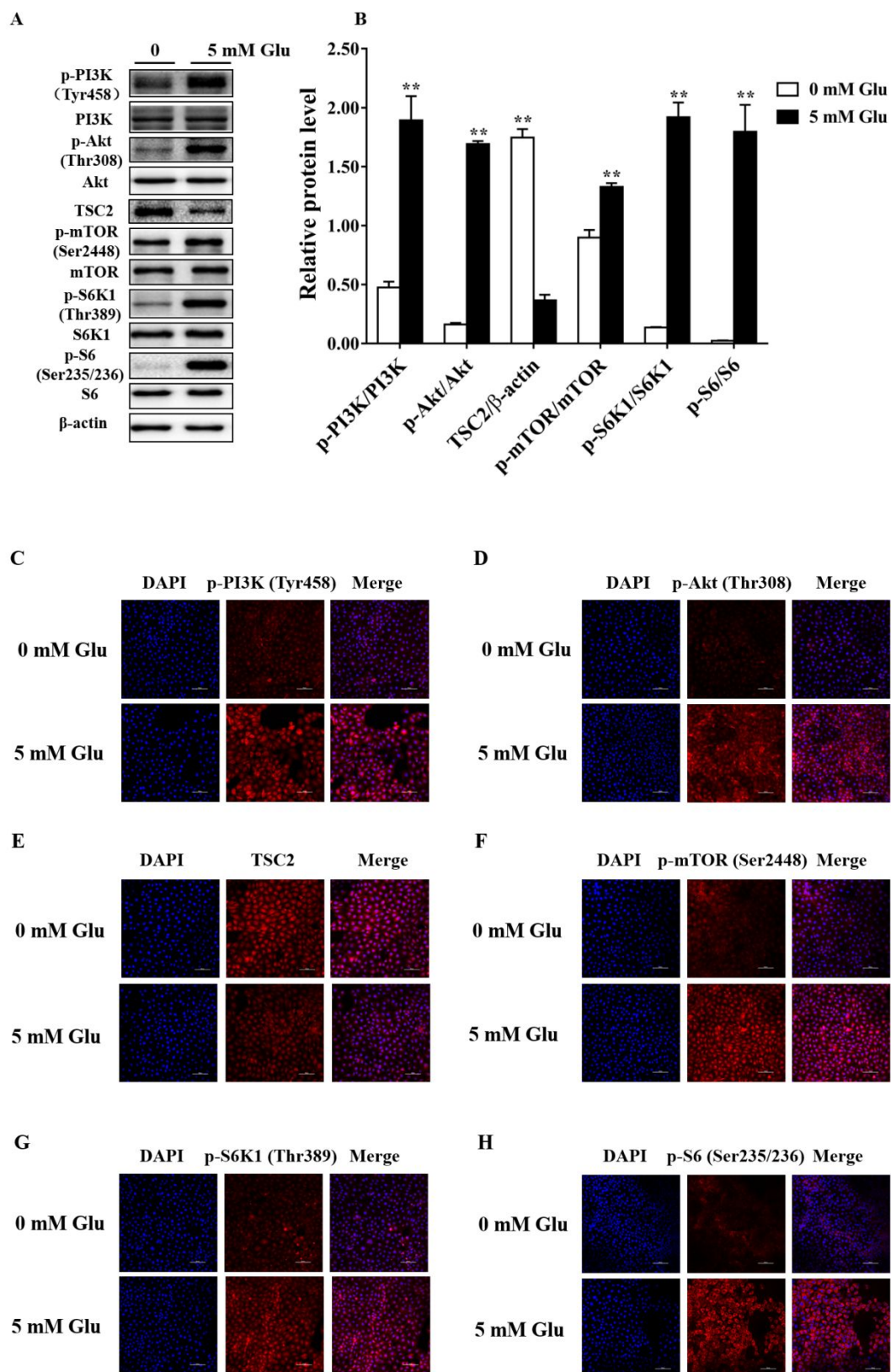
Figure 4. Glu activated the PI3K/Akt pathway. A. IPEC-J2 cells were serum-starved for 15 h, amino acid-starved for 4 h and then treated with 0 or 5 mM

Glu for 60 min. Western blotting analysis showed the effect of 5 mM Glu on the levels of the following PI3K/Akt signaling proteins: p-PI3K, PI3K, p-Akt, Akt, and TSC2. The phosphorylation of mTOR, S6K1, and S6 was analyzed. B. Quantification was performed by measuring the intensity of each band by densitometry using ImageJ software. The results are representative of three independent experiments and are reported as the mean ± SEM. ** indicates $P < 0.01$. C-H. Representative immunofluorescence images of 0 or 5 mM Glu-treated cells labeled with DAPI (blue) and target protein antibodies (red). Scale bar: 100 μm.
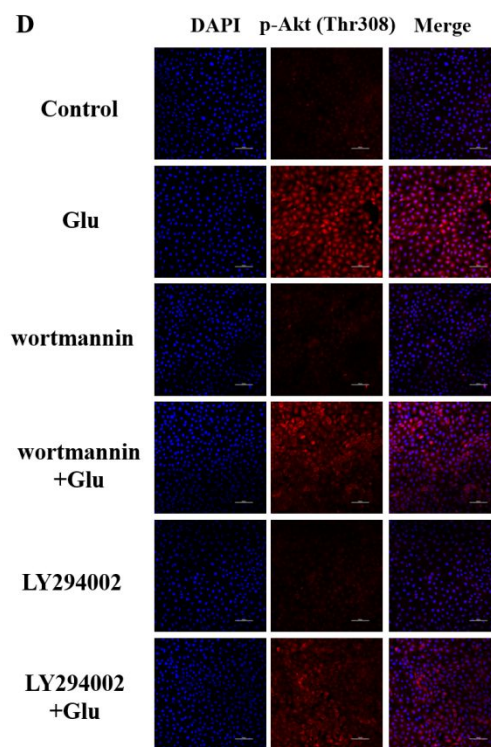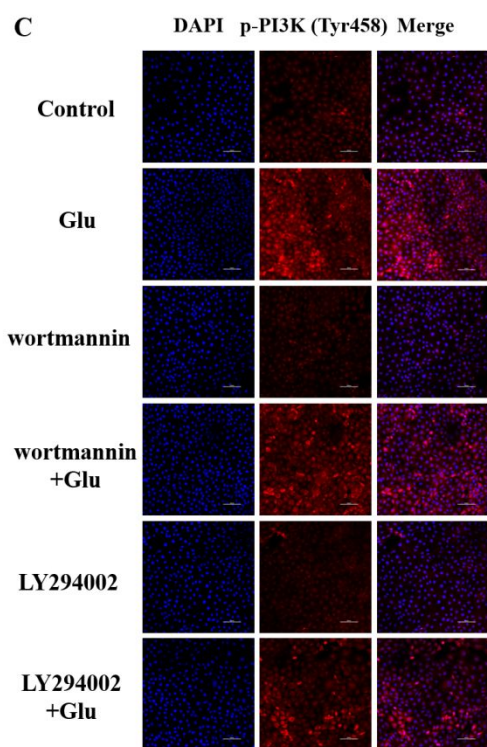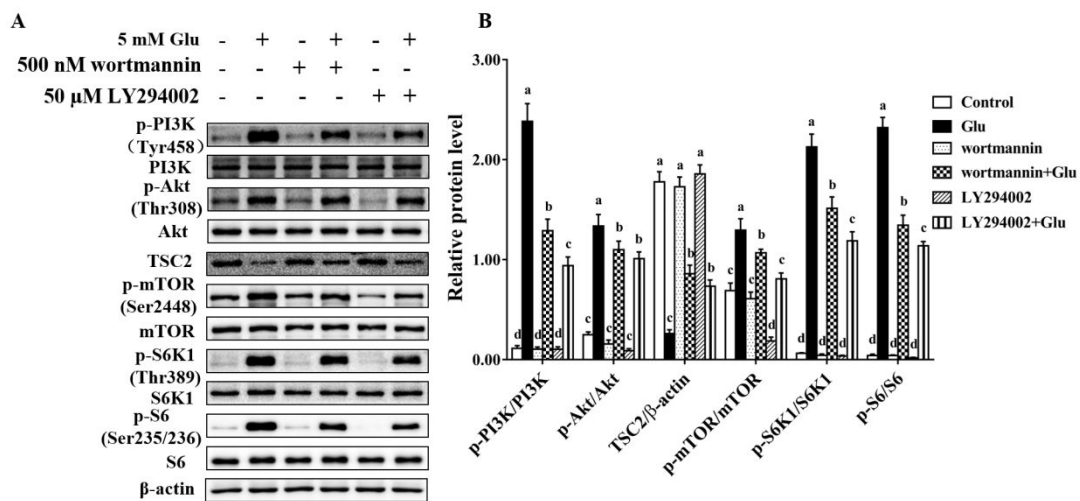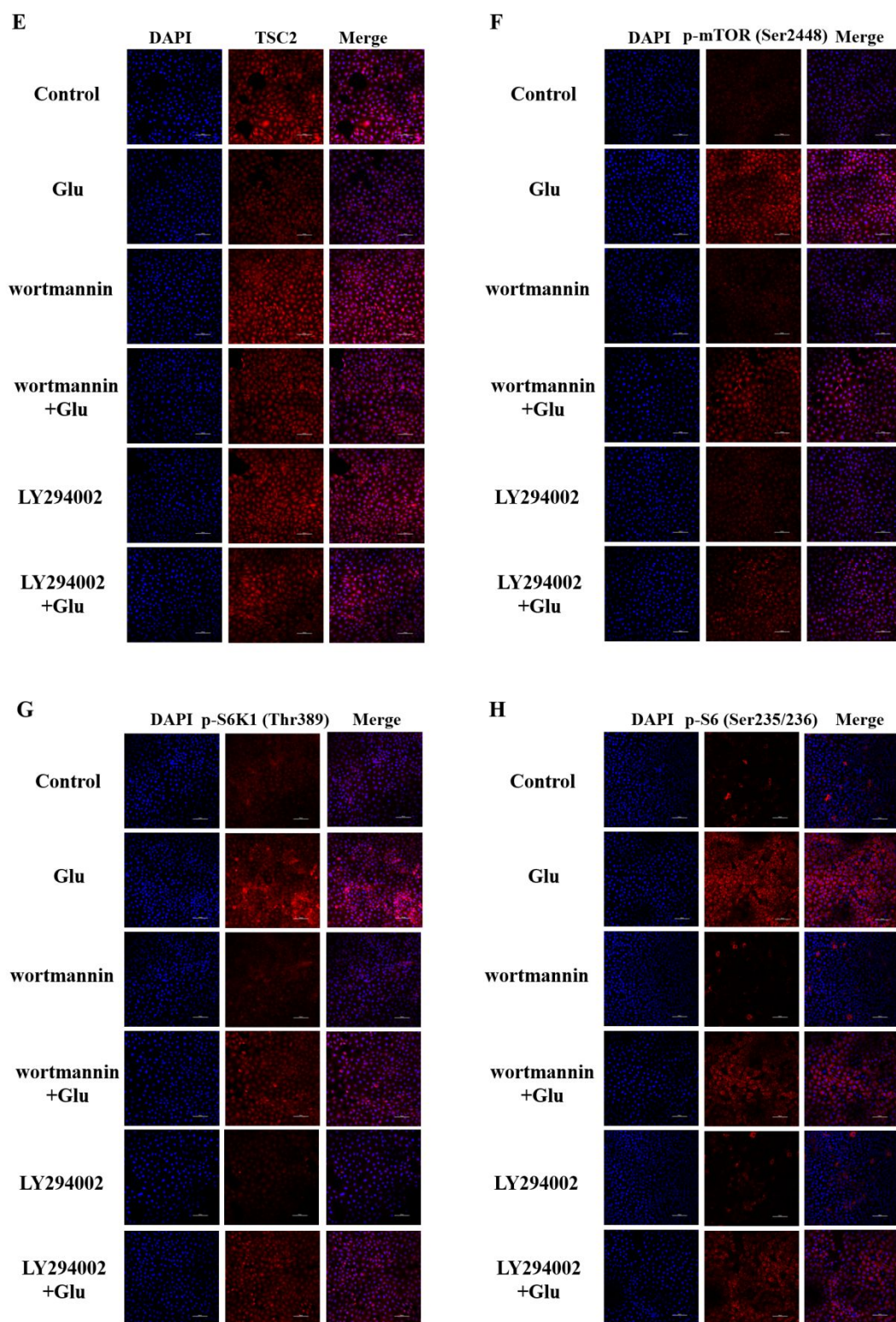
Figure 5. PI3K inhibition partially reduced Glu-induced PI3K/Akt/mTORC1 pathway activation. After starvation, the control (0.1% DMSO), Glu, wortmannin, LY294002, wortmannin + Glu, and LY294002 + Glu groups were treated with HBSS,

5 mM Glu, 500 nM wortmannin, 50 μM LY294002, 500 nM wortmannin + 5 mM Glu, and 50 μM LY294002 + 5 mM Glu, respectively, for 60 min. A. Western blotting was used to analyze the levels of p-PI3K, PI3K, p-Akt, Akt, TSC2, p-mTOR, mTOR, p-S6K1, S6K1, p-S6, and S6. B. Quantification was performed by measuring the intensity of each band by densitometry using ImageJ software. The results are representative of three independent experiments and are reported as the mean ± SEM. In the bar charts, different superscript small letters indicate significant differences ($P < 0.05$), while the same letters represent no significant difference ($P > 0.05$). C-H. Immunofluorescence staining was used to examine changes in p-PI3K, p-Akt, TSC2, p-mTOR, p-S6K1, and p-S6 expression under the treatment of Glu, wortmannin or LY294002. Control: 0 mM Glu (0.1% DMSO), Glu: 5 mM Glu, wortmannin: 500 nM wortmannin, LY294002: 50 μM LY294002, wortmannin + Glu: 500 nM wortmannin + 5 mM Glu, and LY294002 + Glu: 50 μM LY294002 + 5 mM Glu. Scale bar: 100 μm.
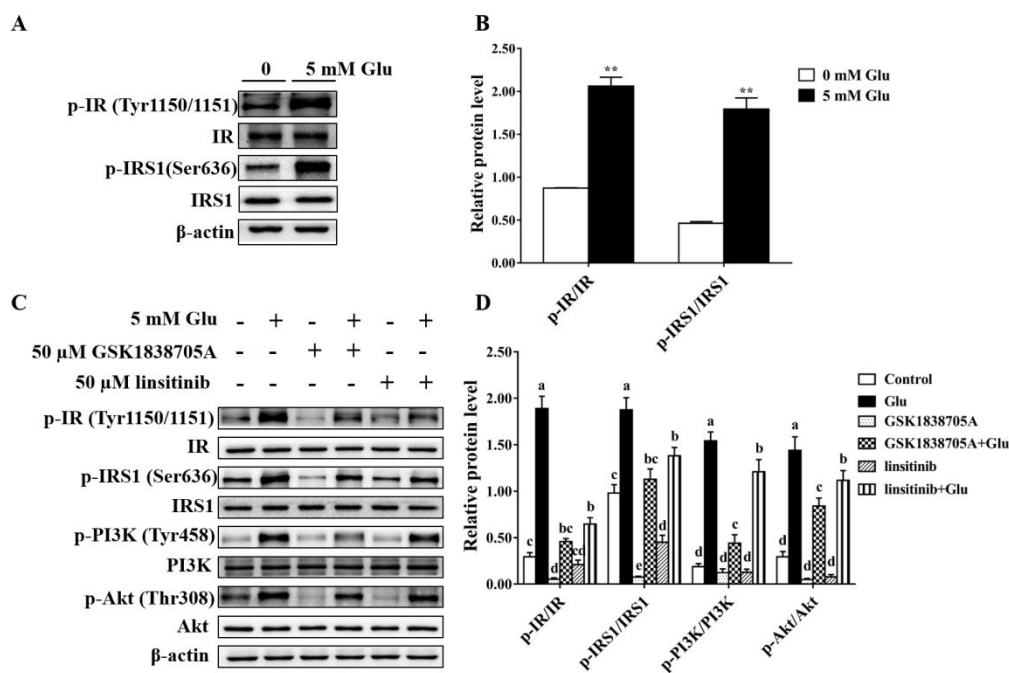
Figure 6. The insulin receptor is involved in Glu-induced mTORC1 activation.
A. IPEC-J2 cells were serum-starved for 15 h, amino acid-starved for 4 h and then treated with 0 or 5 mM Glu for 60 min. Western blotting analysis showing the effect of 5 mM Glu on the levels of the following IR/IRS signaling proteins: p-IR, IR, p-IRS1, IRS1. B. Quantification was performed by measuring the intensity of each band by densitometry using ImageJ software. C-D. Insulin receptor inhibitors depressed IR/IRS/PI3K/Akt signaling. After starvation, the control, Glu, GSK1838705A, GSK1838705A + Glu, linsitinib, and linsitinib + Glu groups were treated with HBSS, 5 mM Glu, 50 μM GSK1838705A, 50 μM GSK1838705A + 5 mM Glu, 50 μM linsitinib, and 50 μM linsitinib + 5 mM Glu, respectively, for 60 min. C. Western blotting was used to analyze the expression levels of p-IR, IR, p-IRS1, IRS1, p-PI3K, PI3K, p-Akt, and Akt. D. Quantification was performed by measuring the intensity of each band by densitometry using ImageJ software. The results are representative of three independent experiments and are reported as the mean ± SEM. ** indicates $P < 0.01$ between groups. In the bar charts, different superscript small

letters indicate significant differences ($P < 0.05$), while the same letters represent no significant difference ($P > 0.05$). Control: 0 mM Glu (0.1% DMSO), Glu: 5 mM Glu, GSK1838705A: 50 μM GSK1838705A, linsitinib: 50 μM linsitinib, GSK1838705A + Glu: 50 μM GSK1838705A + 5 mM Glu, and linsitinib + Glu: 50 μM linsitinib + 5 mM Glu.
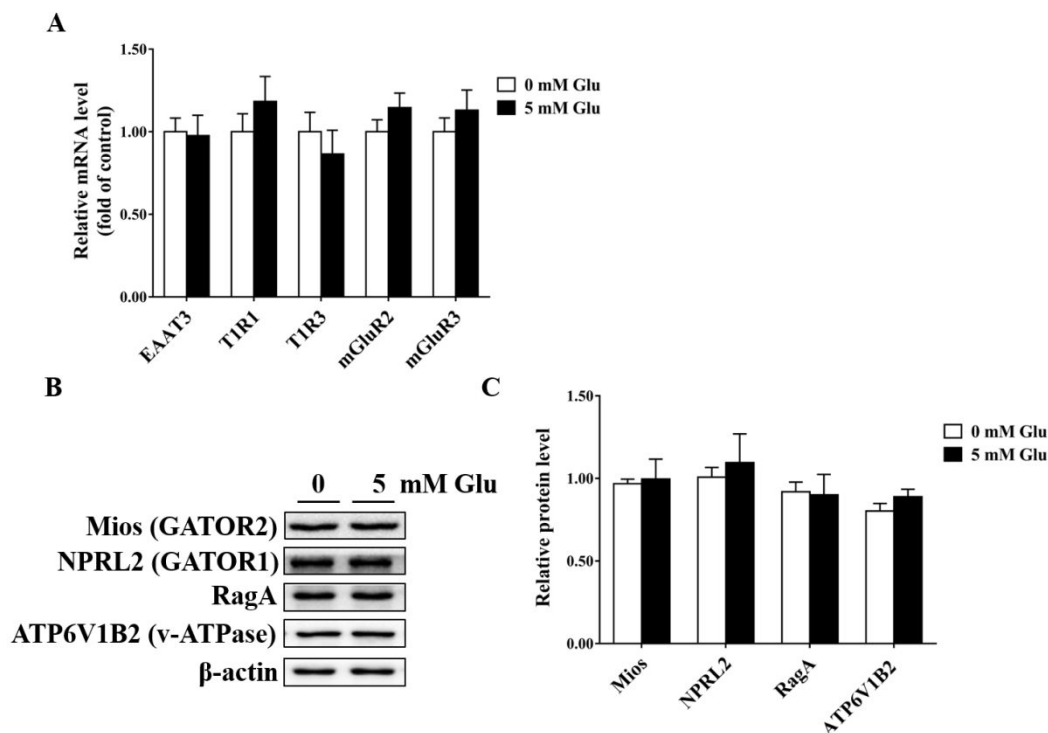
Figure 7. A Glu transporter, Glu receptors and GATOR2/GATOR1/Rag GTPase signaling were not changed during Glu-induced mTORC1 activation. A. IPEC-J2 cells were serum-starved for 15 h, amino acid-starved for 4 h and then treated with 0 or 5 mM Glu for 60 min. The cells were collected to determine the mRNA abundance of the genes of interest using a real-time polymerase chain reaction. B. Western blotting was used to analyze the levels of Mios (GATOR2), NPRL2 (GATOR1), RagA, and ATP6V1B2 (v-ATPase). β-actin was used as a loading control. C. Quantification was performed by measuring the intensity of each band by densitometry using ImageJ software. The results are representative of three independent experiments and are reported as the mean ± SEM. Representative results of three independent experiments are shown. The bars indicate the means ± SEM.
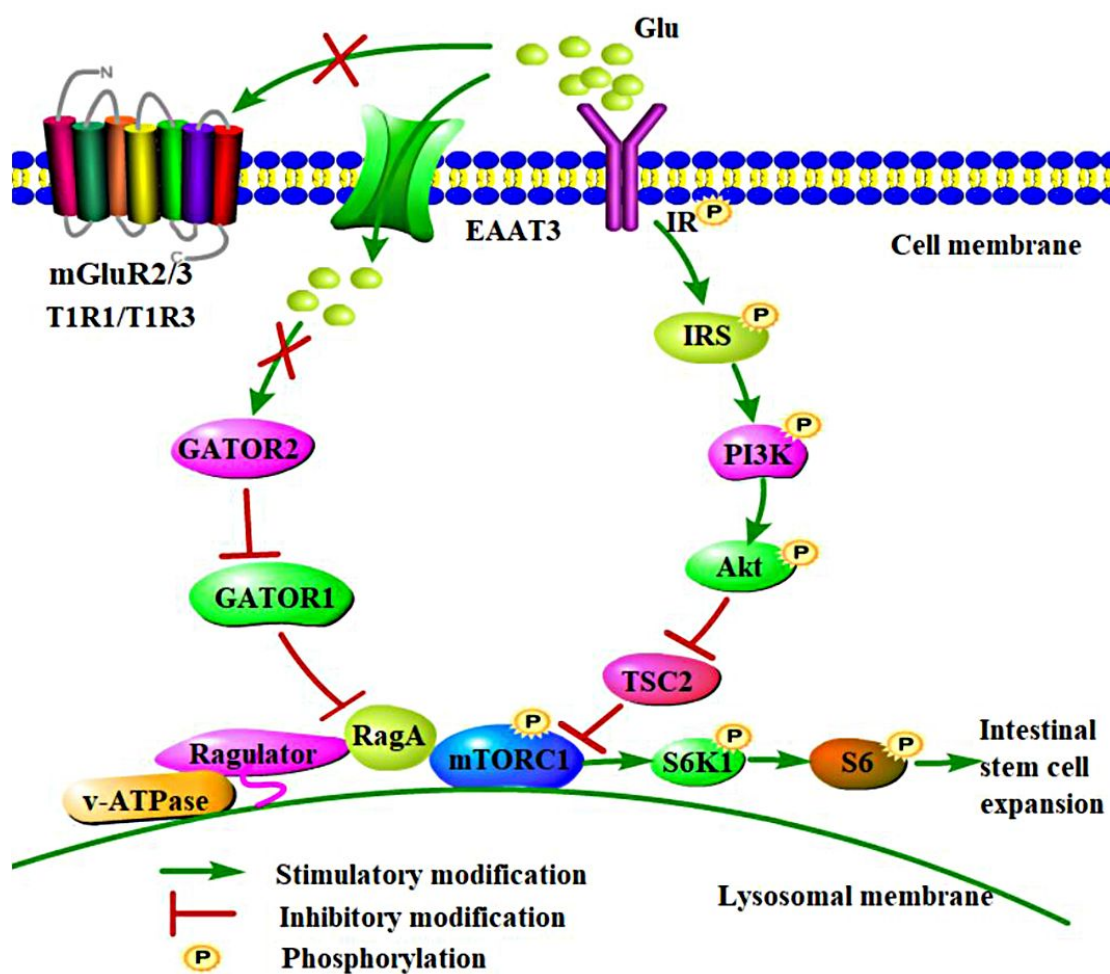
Figure 8. Glu induced mTORC1 activation in the intestinal epithelium. Glu activates mTORC1 through the IR/IRS/PI3K/Akt signaling pathway and promotes intestinal stem cell expansion. The expression of EAAT3, T1R1/T1R3, mGluR2/3, GATOR2, GATOR1, RagA, and v-ATPase did not change after extracellular Glu stimulation.